

# DETECTING THE PRESENCE OF AN INHOMOGENEOUS REGION IN A HOMOGENEOUS BACKGROUND: TAKING ADVANTAGES OF THE UNDERLYING GEOMETRY VIA MANIFOLDS

Xiaoming Huo & Jihong Chen

School of Industrial & System Engineering,  
Georgia Institute of Technology,  
Atlanta, GA 30332

## ABSTRACT

Detection of inhomogeneous regions in a homogeneous background (e.g. textures) is considered. The underlying assumption is that samples from the homogeneous background reside on an underlying manifold, while samples that intersect with the embedded object (i.e. the inhomogeneous region) are ‘away’ from this manifold. The empirical distance from each sample (which will be specified in the paper) to the manifold is a quantity to determine the likelihood of a sample’s overlapping with an embedded object. This result can consequently be integrated with the ‘Significant Runs Algorithms’, to predict the presence of embedded structures. A ‘local projection’ algorithm is designed to estimate the distances between samples and the manifold. Simulation results for features embedded in textural imageries show promises. This work can be extended to a formal theoretical framework for underlying feature detection. It is particularly suitable for textural images.

## 1. INTRODUCTION

We consider detecting objects in a homogeneous background. The *objects* are regions within which the distributional properties of these image pixels are different from those in the rest of the image. Two exemplary cases are given in Figure 1 and 2; in each case, there is a textural image, a trigonometric-function-shaped slim regions with contents different from the texture, and a combination of both of them. The detection problem is (1) to determine the presence of a object region, and furthermore (2) to infer the location and shape of the object region.

This problem is a fundamental problem in many applications, such as target recognition, satellite image processing, and so on.

In this paper, we explore the following idea: (1) the background makes the majority of an image, while a object region is the ‘minority’; (2) In addition, the majority of the images (from the homogeneous background), if appropriately sampled, are located in a low-dimensional manifold; (3) For samples that overlap with the embedded region, they are ‘away’ from the manifold. Given that the above three conjectures are true, the distance from a sampled patch to the underlying manifold gives the probability that a sample overlaps with the embedded object. If all the *high probability samples* are relative concentrated, then one has

This work has been partially supported by National Science Foundation grants DMS 01-40587 and DMS 03-46307. Copyright 2003 IEEE. Published in the Proceedings of International Conference on Acoustic Signal and Speech Processing, May, 17-21, 2004, Montreal, Quebec, CANADA.

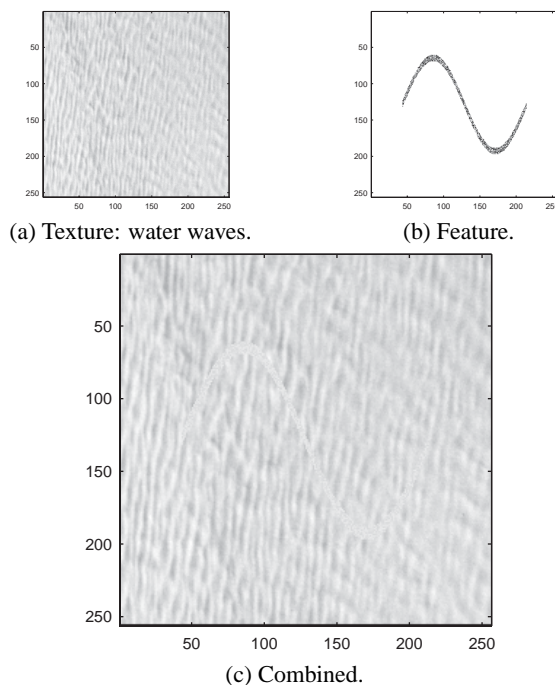


**Fig. 1.** Example of a object (shaped like a trigonometric function, with its own textural distribution, as depicted in figure (b)) that is embedded in a textural image (figure (a)). Figure (c) is the combination: (c)=(a)+(b).

evidence for the presence of an embedded object; otherwise there may not be an embedded object. An illustration of an underlying manifold for samples (e.g., patches) from a homogeneous background is given in Figure 3. A previously developed framework named *significantly run algorithms* [1, 2, 3] can be used to process the patterns of the high probability samples. The distance from a sample to an underlying manifold can be empirically estimated by an algorithm—Local Linear Projection (LLP)—that is designed in other occasions [4, 5]. The principal idea of LLP is inspired by LLE [6] and ISOMAP [7]. Simulations demonstrated the effectiveness of this approach.

The rest of this paper is organized as follows. In Section 2, the formulation of the problem is given. In Section 3, the distance to a manifold is defined. In Section 4, the Local Linear Projec-

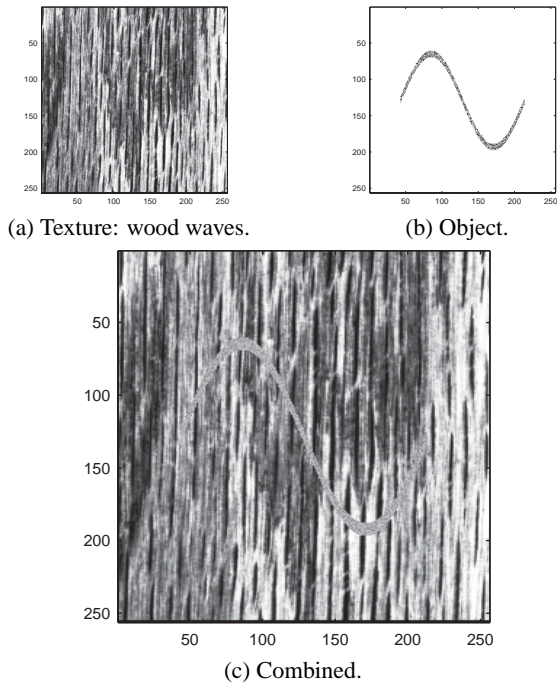


Fig. 2. Another example of embedded object.

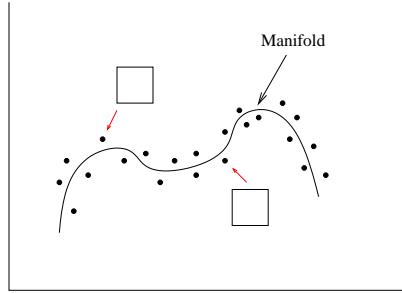


Fig. 3. An illustration of the presence of a manifold.

tion algorithm is described. Section 5 describes the Significance Run Algorithm (SRA). In Section 6, some issues in parameter estimation are discussed. In Section 7, we present simulation results. Some discussions are presented in Section 8. Finally, we conclude in Section 9.

## 2. FORMULATION

For an  $N$  by  $N$  image, let  $y_i, i \in \mathcal{I}$ , denote all of the  $8$  by  $8$  sampled patches with two diagonal corners being at  $(4a+1, 4b+1)$  and  $(4a+8, 4b+8)$ , where  $0 \leq a, b \leq (N-8)/4$ . The patch size  $(8 \times 8)$  is chosen for computational convenience. We assume that if patch  $y_i$  is sampled in the background, then

$$y_i = f(t_i) + \varepsilon_i, \quad i \in \mathcal{I},$$

where function  $f(\cdot)$  is a locally smooth function that determines the underlying manifold,  $t_i$ 's denote the underlying parameters for the manifold, and  $\varepsilon_i$ 's are random errors.

## 3. DISTANCE TO MANIFOLD

For any patch,  $y_i$ , the distance from this patch to its original image on the manifold, which is  $f(t_i)$ , is

$$\|y_i - f(t_i)\|_2. \quad (1)$$

As explained earlier, this distance measures how likely the patch is in the background. The larger the above distance is, the less likely this patch is on the background. An illustration of the distance

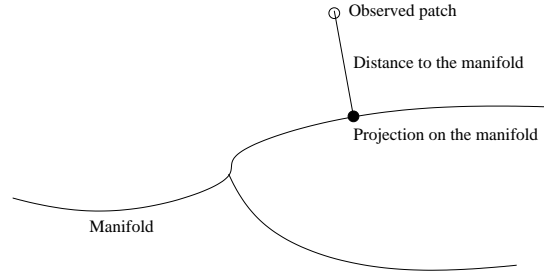


Fig. 4. An illustration of distance from an observed patch to the manifold.

from a patch to the manifold is given in Figure 4. Note that function  $f(\cdot)$  is not available. In the next section, a numerical method is designed to estimate this distance.

## 4. LLP: LOCAL LINEAR PROJECTION

An LLP can be applied to extract the local low-dimensional structure. In the first step, neighboring observations are identified. In the second step, a Singular Value Decomposition (SVD) or a Principal Component Analysis (PCA) is used to estimate the local linear subspace. Finally, the observation is projected into this subspace. An illustration of LLP in 2-D with local dimension being equal to 1 (i.e., linear) and 15 nearest neighbors is provided in Figure 5. A detailed description of the algorithm is given in the

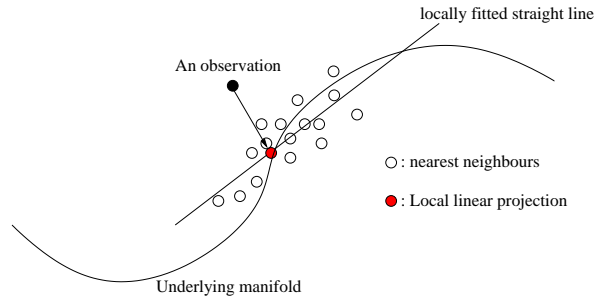


Fig. 5. An illustration of Local Linear Projection in a 2-D space with local dimension being equal to 1 and 15 nearest neighbors.

following.

---

### ALGORITHM: LLP

**for** each observation  $y_i, i = 1, 2, 3, \dots, N$ ,

1. Find the  $K$ -nearest neighbors of  $y_i$ . The neighboring points are denoted by  $\tilde{y}_1, \tilde{y}_2, \dots, \tilde{y}_K$ .
2. Use PCA or SVD to identify the linear subspace that contains most of the information on vectors  $\tilde{y}_1, \tilde{y}_2, \dots, \tilde{y}_K$ . Suppose the linear subspace is  $\mathcal{A}_i$ , and  $P_{\mathcal{A}_i}(x)$  denote the projection of a vector  $x$  into this subspace. Let  $k_0$  denote the assumed dimension of the embedded manifold, then subspace  $\mathcal{A}_i$  can be viewed as a linear subspace spanned by the vectors associated with the first  $k_0$  singular values.
3. Project  $y_i$  into the linear subspace  $\mathcal{A}_i$  and let  $\hat{y}_i$  denote this projection:  $\hat{y}_i = P_{\mathcal{A}_i}(y_i)$ .

end.

---

The distance between  $y_i$  ( $i \in \mathcal{I}$ ) and  $f(t_i)$  can be estimated by  $\|y_i - \hat{y}_i\|_2$ .

## 5. SRA: SIGNIFICANT RUN ALGORITHM

Even though the distance to a manifold can be estimated, it still remains unclear when the distance is *significantly* large. Instead of studying the distribution of the distances themselves, we study their spatial patterns by using a *significance run algorithm* (SRA), which was introduced in [1], and was later used in [2] and [3].

A summary of a SRA is as follows. Each patch is associated with a node. Because patches are equally spaced, they form a table like in Figure 6. There is an edge between two nodes iff their cor-

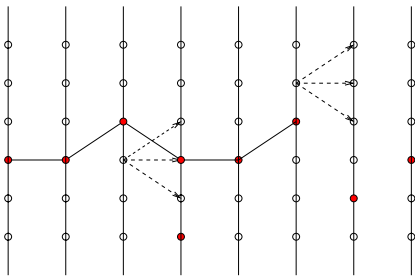


**Fig. 6.** An illustration of Significance Graph and a Significance Run.

responding patches are spatially connected. A node is significant iff the corresponding distance  $\|y_i - \hat{y}_i\|_2$  is above a prescribed threshold (denoted by  $\mathcal{T}_1$ ). A *significance run* is a chain of connected significant nodes. The length of the longest significance run is the test statistic: an embedded object is claimed to be present iff this length is above a constant (denoted by  $\mathcal{T}_2$ ). It has been shown in other occasions (e.g., [1, 3]) that SRA leads to a powerful test.

Note that both  $\mathcal{T}_1$  and  $\mathcal{T}_2$  can be determined numerically. Constant  $\mathcal{T}_1$  can be a given percentile of the empirical estimates of the distances:  $\|y_i - \hat{y}_i\|_2$ . Constant  $\mathcal{T}_1$  can be derived from simulations.

## 6. PARAMETER ESTIMATION

In the LLP, one needs to specify the number of nearest neighbors and the local dimension. This can be done by studying the empirical distribution of the distances and the total residual sums of squares.

### 6.1. Number of Nearest Neighbors

An illustration of the percentiles of the distances to the nearest neighbors are given in Figure 7. We choose 50 nearest neighbors,

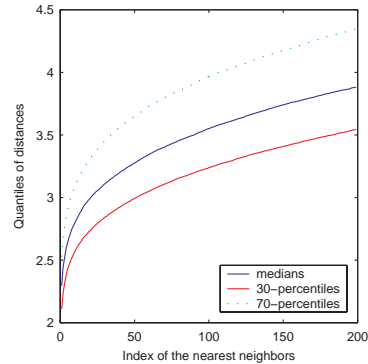


**Fig. 7.** Percentiles of the distances from the nearest neighbors.

because it is approximately a kink point in this figure. It is possible to choose the number of nearest neighbors by studying the distances to the nearest neighbors. In this paper, we do not pursue in this direction.

### 6.2. Local Dimension

The problem of estimating local dimensionality has been analyzed in [6] and [7]. There are followup works in this line. Due to space, we omit the details. Figure 8 gives the plot of the residual sums of squares ( $\sum_{i \in \mathcal{I}} \|y_i - \hat{y}_i\|_2^2$ ) versus the local dimensions (as  $k_0$  in the LLP). An approximate kink point is at  $k_0 = 15$ , which is our

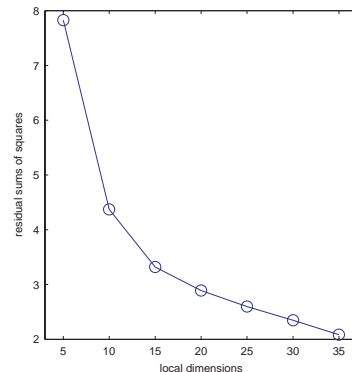


**Fig. 8.** Residual sum of squares versus local dimensions.

choice of local dimension in Simulations.

## 7. SIMULATIONS

We apply the above approach to the two figures in Figure 1 (c) and Figure 2 (c). The positions of the significant patches are displayed in Figure 9 (for the water image) and in Figure 10 (for the wood image) respectively. In both cases, the constant  $\mathcal{T}_1$  is chosen to be the 95th percentile of the squared distances:  $\|y_i - \hat{y}_i\|_2^2, \forall i \in \mathcal{I}$ . Obviously, the significant patches are concentrated around the

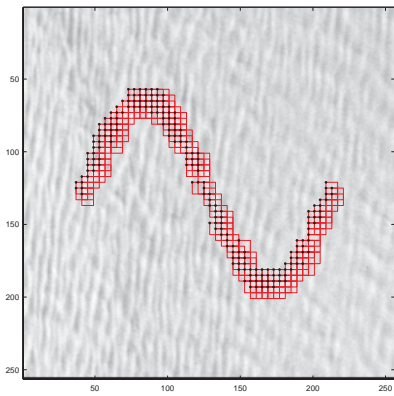


**Fig. 9.** Pattern of significant patches for water image. Northwest corners of significant patches are marked by dark dots.

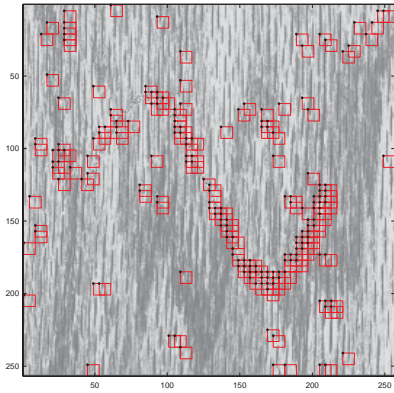


**Fig. 10.** Pattern of significant patches for wood image. Northwest corners of significant patches are again marked by dark dots.

embedded object, which is the trigonometric shape. Hence a SRA will unveil the presence of the object.

For comparison, Figure 11 gives the patterns of significant patches when there is no embedded objects.

## 8. DISCUSSION

By modifying the structure of the significant graph, the above approach can be generalized for more general object, e.g., instead of functions, one can consider curves, or even non-filamentary objects. We leave this as a future work.

If the background is non-homogeneous, which is true in many cases, then the above approach will fail. The proposed framework can be utilized to derive a general theory on when an embedded object is detectable, and when it is not. This will be another future work.

## 9. CONCLUSION

A framework that utilizes the underlying geometric distribution is proposed to detect objects in a homogeneous background. Simulations showed the promises of the proposed method. The proposed method takes advantages of an underlying manifold, on which the

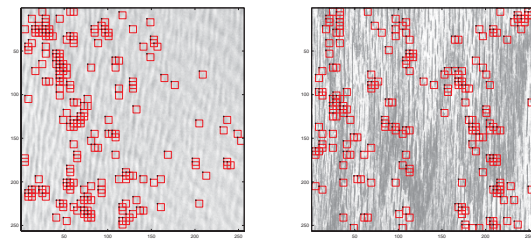


**Fig. 11.** Pattern of significant patches for water and wood image, while there is no embedded object.

sampled patches from the image reside. Significant Run Algorithm is utilized to generate a hypothesis testing procedure.

## 10. REFERENCES

- [1] E. Arias, D. L. Donoho and X. Huo (2003). Adaptive multiscale detection of filamentary structures embedded in a background of Uniform random points. *Tech. Report*. Stanford University. <http://www-stat.stanford.edu/~donoho/reports.html>.
- [2] X. Huo, J. Chen, and D.L. Donoho (2003). Multiscale Detection of Filamentary Features in Image Data. *SPIE Wavelet-X*, San Diego, CA, August.
- [3] X. Huo, J. Chen, and D.L. Donoho (2003). Multiscale Significance Run: Realizing the ‘Most Powerful’ Detection in Noisy Images. *Asilomar Conference on Signals, Systems, and Computers*, November, 9-12, Pacific Grove, CA.
- [4] X. Huo (2003). A geodesic distance and local smoothing based clustering algorithm to utilize embedded geometric structures in high dimensional noisy data. *SIAM International Conference on Data Mining, Workshop on Clustering High Dimensional Data and its Applications*. San Francisco, CA, May.
- [5] X. Huo, and J. Chen (2002). Local Linear Projection (LLP). *First IEEE Workshop on Genomic Signal Processing and Statistics (GENSIPS)*, Raleigh, NC. October 11-13. <http://www.gensips.gatech.edu/proceedings/>.
- [6] S.T. Roweis, and L.K. Saul (2000). Nonlinear dimensionality reduction by locally linear embedding. *Science*, vol 290: 2323-2326.
- [7] J.B. Tenenbaum, V. Silva, and J.C. Langford (2000). A global geometric framework for nonlinear dimensionality reduction. *Science*, vol 290: 2319-2323.